Proceedings of the 2016 IEEE International Conference on
Simulation, Modeling, and Programming for Autonomous Robots
San Francisco, USA, Dec 13-16, 2016

Optimizing Grippers for Compensating Pose Uncertainties by Dynamic Simulation

Adam Wolniakowski[1], Aljaž Kramberger[2], Andrej Gams[2], Dimitrios Chrysostomou[3], Frederik Hagelskjær[4], Thomas Nicky Thulesen[4], Lilita Kiforenko[4], Anders Glent Buch[4], Leon Bodenhagen[4], Henrik Gordon Petersen[4], Ole Madsen[3], Aleš Ude[2], Norbert Krüger[4]

***Abstract*— Gripper design process is one of the interesting challenges in the context of grasping within industry. Typically, simple parallel-finger grippers, which are easy to install and maintain, are used in platforms for robotic grasping. The context switches in these platforms require frequent exchange of gripper fingers to accommodate grasping of new products, while subjected to numerous constraints, such as workcell uncertainties due to the vision systems used. The design of these fingers consumes the man-hours of experienced engineers, and involves a lot of trial-and-error testing.**

In our previous work, we have presented a method to automatically compute the optimal finger shapes for defined task contexts in simulation. In this paper, we show the performance of our method in an industrial grasping scenario. We first analyze the uncertainties of the used vision system, which are the major source of grasping error. Then, we perform the experiments, both in simulation and in a real setting. The experiments confirmed the validity of our approach. The computed finger design was employed in a real industrial assembly scenario.

I. INTRODUCTION

Grasping based on pose estimation using vision has to deal with vision induced uncertainties. These uncertainties are related to the quality of the generated point cloud, the sensor choice, the geometrical relation of the sensor to the object and the number of sensors used. Often, a rough estimate of the uncertainty imposed by the vision system can be found in the form of positional and angular uncertainties by simply analyzing the variance of different pose estimate samples under naturally occurring illumination conditions.

Assuming that an estimate of the vision induced uncertainty exists, the gripper design can be chosen to compensate for the expected pose uncertainties by introducing a cutout in the robot finger (see Fig. 1). Different types of such cutouts exist, such as cutouts based on molding ("inverse" of the object) [1], convex hulls [2], or simple geometric primitives (prismatic, round). In [3], it was shown how to learn optimal finger parameters for two-finger grippers in simulation, where one of the objectives was to enhance the gripper's alignment capability.

In this work, we describe an application in which first rough estimates of visual uncertainties are made for two pose estimation tasks (see Fig. 6). We then compute grippers that compensate for these uncertainties in simulation (see Fig. 3). To verify the alignment capabilities of the computed grippers, we have applied the gripper design in a real world experiment on a test platform (see Fig. 8 and 9). We then integrate the computed cutouts in a gripper that is supposed to handle a number of grasping tasks (see Fig. 4) and applied it in an industrial application context.

By that, we have closed the circle between vision induced uncertainties, gripper design and required alignment properties. Hence our methodology allows for simplifying the set-up of robot assembly systems, by replacing the design problem of grippers by an automatic procedure based on uncertainty estimation from vision, gripper optimization and 3D printing.

II. STATE OF THE ART

In this Section we give an overview of the research previously done in the areas of grasping, gripper design, and the pose estimation using vision systems.

A. Gripper Design in Industry

It is increasingly common for robotic grasping systems to replace manual labour in the industry. These systems have to meet requirements on efficiency and reliability, in order to be economically viable. The gripper design is a critical part of implementing such a robotized solution. Nowadays, it is most common to use parallel-finger grippers in industrial settings. The fingers are developed by experienced engineers, with design choices based on human expertise, and a costly and time-consuming trial-and-error process.

There are various guidelines available to assist in the gripper design problem, i.e. [4]–[7]. They emphasise the reliability of the gripper, increase in the system throughput, and cost optimization. These objectives are often conflicting, but a good compromise can be achieved by minimizing gripper weight, reducing its footprint, including cutouts in

[1]Adam Wolniakowski is with Faculty of Mechanical Engineering, Biaystok University of Technology, 15-351 Biaystok, Poland adam.wolniakowski@gmail.com

[2]Andrej Gams, Aljaž Kramberger, and Aleš Ude are with the Jožef Stefan Institute, 1000 Ljubljana, Slovenia {aljaz.kramberger, andrej.gams, ales.ude}@ijs.si

[3]Dimitrios Chrysostomou, and Ole Madsen are with the Aalborg University, DK-9220 Aalborg East, Denmark {dimi, om}@m-tech.aau.dk

[4]Frederik Hagelskjær, Thomas Nicky Thulesen, Lilita Kiforenko, Anders Glent Buch, Leon Bodenhagen, Henrik Gordon Petersen, and Norbert Krüger are with the The Maersk Mc-Kinney Moller Institute, University of Southern Denmark, DK-5230 Odense M, Denmark {frhag, tnt, lilita, anbu, lebo, hgp, norbert}@mmmi.sdu.dk

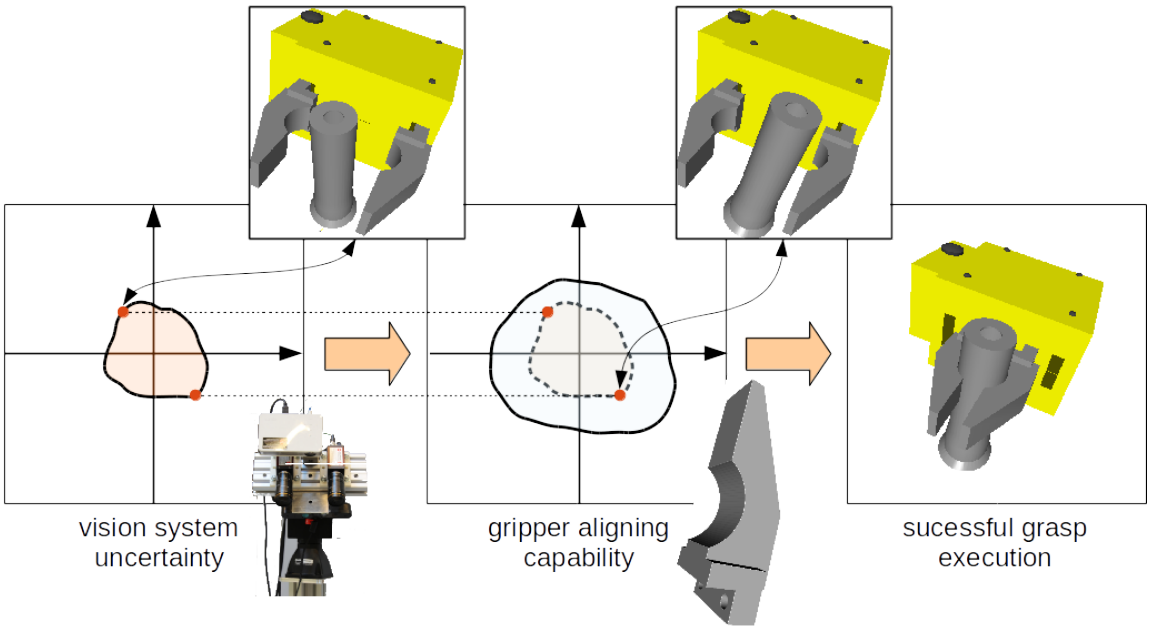

Fig. 1. Overview of the problem. The pose estimation yields inexact results suffering from the uncertainties in the vision systems, which makes the grasping challenging (left). A proper finger design compensates for these uncertainties, resulting in successful grasping (right).

the finger to retain the objects securely, and other similar means.

The gripper jaw design for the purpose of secure grasping and object alignment has also been studied extensively in [8]–[10]. In [10] a parameterization of a modular gripper surface is introduced, and an optimization algorithm to achieve specific object alignment is presented. In [2], the convex-hull based finger shapes are investigated in terms of alignment.

Recently, Schunk GmbH has made an online tool available [1], which can generate finger shapes based on the object molding for simple grasping scenarios.

B. Gripper Learning in Simulation

Simulation as a tool in the context of grasping and gripper design is mostly encountered in problems of optimal grasp planning and structural design [11], [12]. In our previous research, we have used dynamic simulation to obtain feedback in the finger geometry design phase [3], [13]. In this work, using an approach similar to [2], we aim at confirming the relevance of such feedback by presenting and comparing results obtained from the experiments performed in both simulated and the real-world settings.

C. Pose Estimation

The Microsoft Kinect and similar (e.g. Carmine) sensors became popular in computer vision community since the launch in November 2010, because they allow us to extract the RGB and depth information fast and at a low cost. Kinect cameras are not designed with the focus of precision, they are designed for gaming or other human-computer interaction. Therefore it comes with some limitations, such as sensor noise which introduces depth uncertainties. Several studies have been conducted about the noise and reconstruction uncertainties of Kinect point cloud [14], [15].

A large body of work has been produced over the last three decades with the aim of recognizing and performing pose estimation on 3D objects in point clouds. A notable initial work used the local Spin Image descriptor [16] for finding corresponding regions between the object model and a scene. The same principle of using local surface descriptors has since been heavily revisited [17]–[22]. A recent survey [23] provides a comprehensive overview of available 3D descriptors and recognition systems. Furthermore, extensive evaluations of such methods have been carried out [24].

III. METHODS

In our approach, we first analyze the uncertainties of the pose estimation from the vision system used (Primesense Carmine 1.09 sensor) to define the uncertainties relevant for the grasping task (Sect. III-A). We then use the task context as the input to our finger design optimization method to obtain the optimal finger geometry for the two objects considered: the magnet and the rotorcap (Sect. III-B).

A. Pose Estimation

The pose uncertainty results for the magnet and rotorcap objects were computed with methods based on edges, the shape and a method in which features are combined, as described in [25].

The method uses a combination of different descriptors. For each object, we have a 3D model available. First, we extract both edge and surface points from the scene and object point clouds. Then, for each of the edge/surface points, we compute different descriptors, both using the edge and the surface information. For this experiment we used two local histogram based descriptors - SHOT [22] and Cat3DEdge

TABLE I

POSE UNCERTAINTY RESULT FOR MAGNET AND ROTORCAP OBJECT

Object	Features	Error measure	
		Translation [mm]	Rotation [°]
Magnet	edge	2.426	0.21472
	surface points	3.614	0.46372
	combined	2.430	0.21477
Rotorcap	edge	9.4	4.9976
	surface points	4.9	2.8400
	combined	7.75	11.883

[21]. SHOT is a descriptor that performs well for the objects with rich surface data and Cat3DEdge performs well for planar objects by relying on edge data. For both descriptors and for each object point we find the closest match in a scene - a potential correspondent point. We concatenate two correspondence vectors into one and use it as input for the RANSAC algorithm [26] that provides us a 6D pose of the best match.

The resulting pose uncertainties are presented in Tab. I. The result shows the variance of the pose, by estimation of the object pose in 100 consequential scenes by using only the edge points (Cat3DEdge) descriptor, surface point (SHOT) descriptor and both combined. The error variance of detection using only the edge descriptor is lower compared to the surface descriptor for the magnet object. For the rotorcap object it is opposite. By combining both descriptors, we get a result in-between. It allows us to have a more universal method that on average gives less detection variance. The result also shows a high variance in rotation for the rotorcap object. The reason is that this object is symmetrical and therefore has one degree of freedom along the z-axis.

B. Gripper Design Learning

The optimal gripper design for the objects in the considered industrial scenario (*magnet* and *rotorcap*) has been learned using the methods presented in [3]. We describe the main points of the method below for the sake of completeness.

First, we define an objective function that quantitatively describes the quality of the tested gripper design. Such a function is a weighted product of individual Quality Indices, each representing a different facet of the grasping process [13]:

- **Success Index** S, which is defined as the ratio of successful grasps to all grasps simulated:

$$S = \frac{N_{\text{success}}}{N_{\text{total}}}$$

- **Robustness Index** R, representing the stability of grasp success in the presence of noise. This is calculated by repeating the grasp simulation with a pose perturbation introduced to all grasps which were previously successful. The index is defined as the ratio between the number of successful perturbed grasps N^*_{success} to the number of successful grasps N_{success}:

$$R = \frac{N^*_{\text{success}}}{N_{\text{success}}}$$

- **Alignment Index** A, describing the ability of the gripper to position grasped objects in a determined way. This is calculated by comparing the standard deviation of the pose ${}^{\text{TCP}}_{\text{obj}}T$ distribution before the grasping (σ_{before}) to the standard deviation of the same pose distribution after the grasping (σ_{after}):

$$A = max(0,\, 1 - \frac{\sigma^*_{\text{after}}}{\sigma_{\text{before}}})$$

- **Coverage Index** C, illustrating the versatility of the gripper in executing successful grasps from multiple directions. This is defined as the size of the successful grasp pose space, estimated by comparing the number of the successful grasps filtered iteratively in $SE(3)$ (N_{filtered}) to the number of filtered candidate grasps (N_{samples}). The filtering is done by performing clustering.

$$C = \frac{N_{\text{filtered}}}{N_{\text{samples}}}$$

- **Wrench Index** W, which quantifies the quality of executed grasps in terms of forces necessary to dislodge the object. This is calculated based on the GWS measure [27] (using the average distance to the convex hull of the friction cones at the contect points). The GWS_i is computed for each i-th successful grasp, and the Wrench Index is defined as a mean value:

$$W = \frac{1}{N_{\text{success}}} \sum_{i=1}^{N_{\text{success}}} \text{GWS}_i$$

- **Stress Index** ζ, which describes the structural robustness of the gripper design. It is calculated based on the ratio of the maximum bending stress found in the gripper finger σ_{max} to the stress limit σ_{limit}:

$$\zeta = max(0,\, 1 - \frac{\sigma^*_{\text{max}}}{\sigma_{\text{limit}}})$$

- **Volume Index** V, representing the cost of producing the set of fingers (in terms of volume of the material used). This is calculated using the ratio of the finger geometry volume V_{fingers} to the defined volume limit V_{limit}:

$$V = max(0,\, 1 - \frac{V^*_{\text{fingers}}}{V_{\text{limit}}})$$

The objective function is defined as the weighted product of the indices:

$$Q = f(\mathbf{x}) = (\prod_{i=1}^{m} q_i(\mathbf{x})^{w_i})^{1/\Sigma_{i=1}^{m} w_i}$$

where $\mathbf{q} = [S, R, A, C, W, \zeta, V]$ is the vector of m individual gripper quality indices and w_i are the respective weights. Since in the considered industrial case, we are mostly concerned with the alignment properties of the gripper, we have selected the following weights for the objective function:

$$w_S = 0 \quad w_R = 0 \quad w_A = 1 \quad w_C = 0$$
$$w_W = 1 \quad w_\zeta = 0.01 \quad w_V = 0.01$$

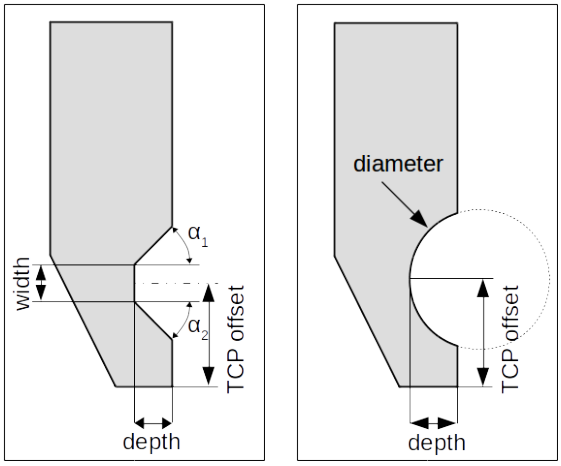

Fig. 2. The parametrization of gripper fingers for the magnet (on the left) and for the rotorcap (on the right).

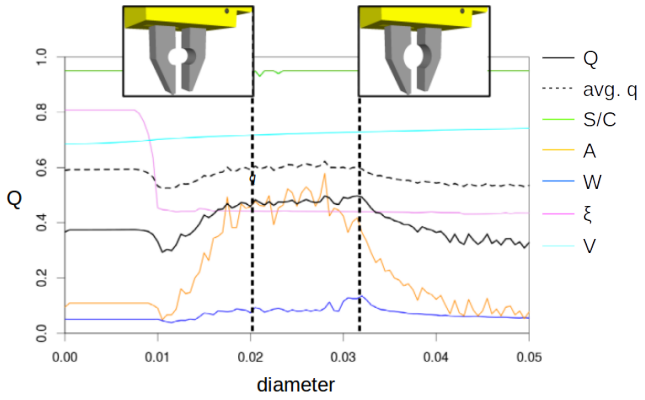

Fig. 3. The final linear search step in the coordinate descent optimization of the *diameter* parameter of the *rotorcap* cutout. The green line shows the value of the *Success Index/Coverage Index*, the orange – *Alignment Index* (w_A), the blue – *Wrench Index* (w_W), the cyan – *Volume Index* (W_V), the pink – *Stress Index* (w_ζ), and the solid black line – the total quality objective.

The assumed limits for the volume and stress are $V_{\text{limit}} = 200\text{cm}^3$ and $\sigma_{\text{limit}} = 25\text{MPa}$ respectively.

We also define several parametrizations of the gripper finger shape (primitive geometry cutouts: prismatic, round, trapezoid). The parametrizations for the magnet cutout (trapezoid shape) and for the rotorcap cutout (round shape) are shown in Fig. 2. The magnet finger is parametrized with the following design variable vector:

$$\mathbf{x}_{\text{magnet}} = [\text{depth, width, TCPoffset, } \alpha_1, \alpha_2]$$

The rotorcap finger is parametrized with the following design variable vector:

$$\mathbf{x}_{\text{rotorcap}} = [\text{depth, diameter, TCPoffset}]$$

The gripper design evaluation is done in an environment simulated using the RobWorkSim simulation framework [28], in which the grasping task from the real-world setting is reproduced with varied perturbations. The grasping task is defined in terms of the gripper open and closed configurations, and the approach direction vector. The gripper approaches the object linearly along the specified vector, and after the grasp is executed the object is lifted vertically. The movement of the gripper base is controlled kinematically. The simulation is done using the underlaying ODE physics engine. The parameters of the simulation have been adjusted so that the grasping is performed in the regime, in which the simulator operates well.

The quantitative design evaluation is subsequently fed into an optimization method, that searches through the parameter space for the optimal configuration. The optimization problem is formulated as:

$$\mathbf{x}_{\text{opt}} = \underset{\mathbf{x} \in \mathbb{R} | \mathbf{x}_{\min} \leq \mathbf{x} \leq \mathbf{x}_{\max}}{\arg\max} f(\mathbf{x})$$

In this work, we have used the *coordinate descent* approach [29] to select the best parameter values. Fig. 3 shows the quality objective values for the *cut width* parameter linear search in the *rotorcap* grasping scenario.

Such procedure was performed for all objects of the industrial assembly scenario within the FP-7 project ACAT (magnet, rotorcap, rotorshaft, and ring). For each of them, we have optimized the individual cutout shape. These cutouts have then been merged into one finger design (see Fig. 4), suitable for all of the objects. In this work, we focus on the *magnet* and *rotorcap* objects, and their corresponding cutouts. The cutout geometry and parameters for the considered objects are presented in Fig. 5.

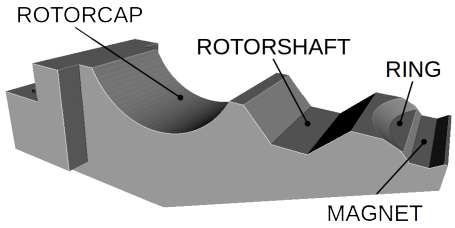

Fig. 4. The combined finger design with four separately learned cutouts for the ACAT objects (magnet, ring, rotorcap, rotorshaft).

Magnet	Rotorcap
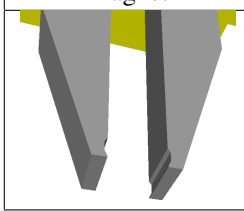	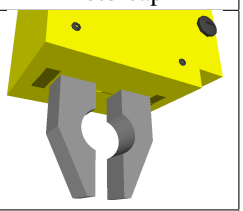
Trapezoid cutout depth: 1 mm width: 2.4 mm TCP off.: 3 mm angle (α_1): 45° angle (α_2): 55°	Round cutout depth: 10 mm diameter: 32.5 mm TCP off.: 45 mm

Fig. 5. Optimal cutout geometries found for the magnet and for the rotorcap.

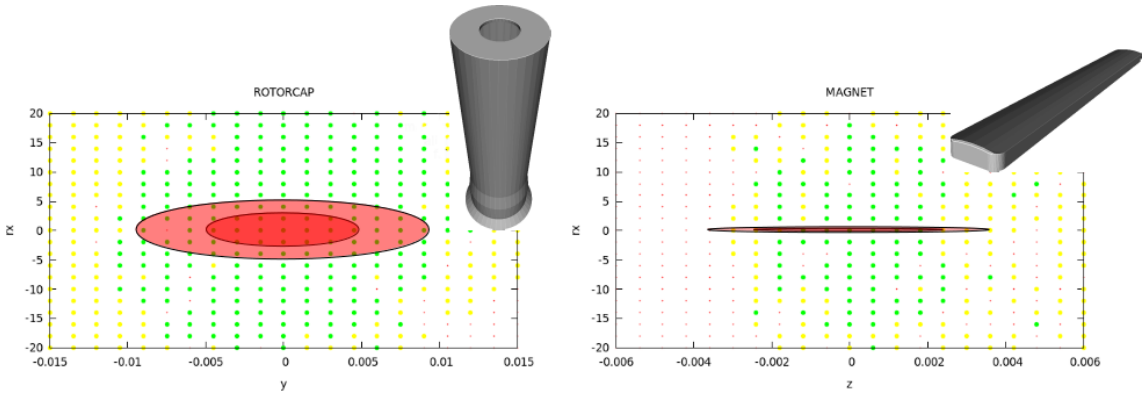

Fig. 6. Basins of convergence for the magnet and for the rotorcap objects for the offsets in selected dimensions. Light red shows the worst case of vision pose estimation uncertainty (see Tab. I – *edge* features for the rotorcap, and *surface points* for the magnet), and dark red indicates the best case (see Tab. I – *surface points* for the rotorcap, and *edge* features for the magnet). Green dots represent the successful grasping area due to the gripper aligning capability.

IV. EXPERIMENTS

In order to validate our approach of gripper finger design, we performed a set of experiments to assess the optimization results quantitatively, and to verify that dynamic simulation matches the observations obtained in the real-life setting. Sects. IV-A and IV-B detail the experimental settings for the two objects considered: the *magnet* and the *rotorcap*. After obtaining the feedback from extensive testing, the computed finger designs were employed in a real grasping scenario on an industrial platform (see Sect. IV-C).

For both objects, we first performed a set of simulations to show their respective *basins of grasping success* (that is, the set of grasp offsets that still result in successful grasping – see Fig. 6). Since exploring these basins would be prohibitively time-consuming, we opted to only test the limits of gripper capabilities along the set of selected cardinal directions in the real-world setting. We argue that such results still provide a good verification of the match between simulation and in-viva experiments.

We performed the grasping experiments using the Kuka LWR-4 robot equipped with a Mitsubishi RH-707 gripper, which we controlled using the Fast Research Interface (FRI) from Matlab. The robot was operating in its stiffest mode. To align the coordinate systems of the object fixtures and the robot, we defined a new, external coordinate system, which is determined with measurements of three positions using the tip of the robot. Experiments on both objects (the magnet and the rotorcap) followed the same procedure. For each of the objects, a *nominal* grasp was defined, which was then perturbed in a structured way. The grasping was tested by placing the gripper in the perturbed pose, closing the fingers, and lifting the object. We have defined three outcomes of that procedure: *success*, *misalignment* (the object is grasped, but in an incorrect pose), and *failure* (the object not grasped, or a collision) based on the qualitative visual assessment (see Fig. 7). Each of the perturbed grasps was repeated 5 times in the real setting.

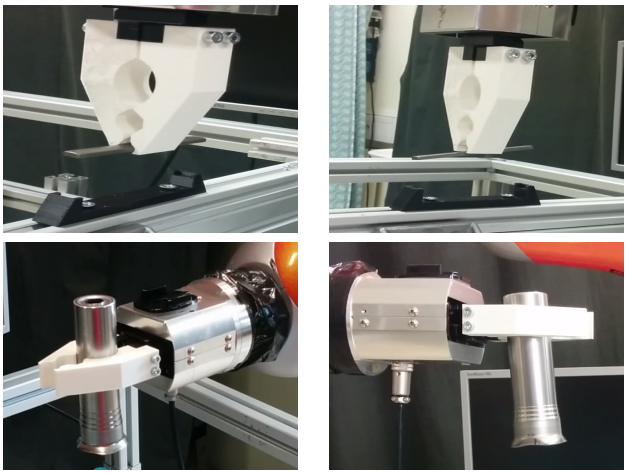

Fig. 7. Qualitative alignment for the tested objects. Top row – from left to right: successful magnet grasp, misaligned magnet grasp. Bottom row – from left to right: successful rotorcap grasp, misaligned rotorshaft grasp.

A. The Magnet

The *magnet* is a small (dimensions: $72 \times 8.2 \times 2.9$ mm, weight: 12 g) metal bar, which has to be inserted into a groove in an electrical motor assembly. Such a procedure imposes tight requirements on grasping and handling precision for this object. Most importantly, the magnet has to be grasped with the distal part of the gripper, so that its designated cutout need to be be located close to the front surface of the fingers. Moreover, the magnet sits in an enclosing fixture which further limits the uncertainty at which the gripper can approach it for the grasping. The real and the simulated fixtures are presented in Fig. 8.

Because of the magnet symmetry, and the fact that an offset in the X direction is less relevant for the handling of the object, we have decided to test the magnet grasping with perturbation in 5 axes (see Tab. II).

Fig. 11 shows a comparison between the results obtained in the real-world experiment (top) and the simulation (bottom). The plots show the outcome probability of the grasp at a given offset in 5 selected axes (where the possible

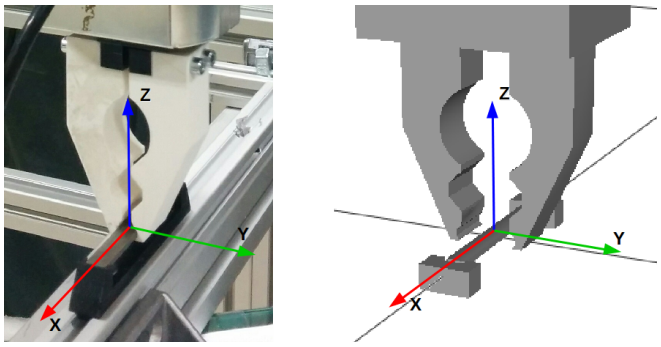

Fig. 8. The magnet object grasping setups: the real setup (left) and the simulated setup (right). The gripper placement indicates the *nominal* grasp defiend for the magnet.

TABLE II

PERTURBATIONS OF THE NOMINAL GRASP FOR THE MAGNET AND THE ROTORCAP SCENARIOS.

Magnet				
Y [mm]	Z [mm]	RX [°]	RY [°]	RZ [°]
$0 \div 6$	$-6 \div 6$	$0 \div 20$	$0 \div 20$	$0 \div 20$
Rotorcap				
X [mm]	Y [mm]	RX [°]	RY [°]	
$0 \div 25$	$-15 \div 15$	$0 \div 45$	$0 \div 45$	

outcomes are success, misalignment, or failure). Smoothed and re-sampled (using linear interpolation) results are shown, since the data points in the real-experiment were not picked uniformly. The grasps were sampled sparsely in the regions of obvious success or failure, and more densely in the are of transition between the two behaviours.

Overall, the simulated and real-world versions of the magnet grasping experiment show decent matches in the Y, Z, and RY axes. The grasping was more successful in the real setting for bigger values of the RZ offset. This can be explained by the compliance in the magnet fixture and the robot, which is not yet modelled in simulation. The wider area of successful grasps in simulated RX offsets is probably due to insufficient modelling of directional friction, encountered in the printed material of the finger.

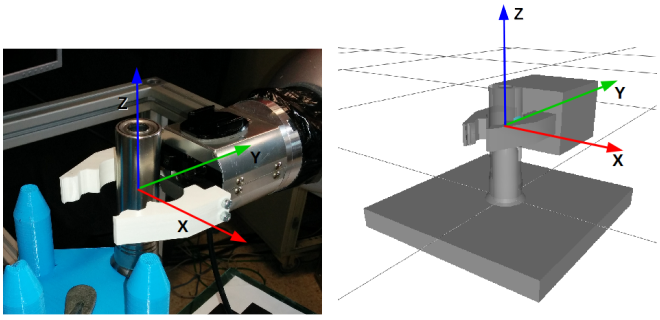

Fig. 9. The rotorcap object grasping setups: the real setup (left) and the simulated setup (right). Fixture on which the rotorcap sits is visible on the left. The gripper placement indicates the *nominal* grasp defined for the rotorcap.

B. The Rotorcap

The *rotorcap* is an aluminum cylindrical object (dimensions: $\oslash 32 \times 110$ mm, weight: 60 g) which is a part of electrical motor assembly that houses the rotor shaft and a set of magnets. The rotorcaps are fed on a fixture, on which the objects sit, and have to be subsequently grasped and placed in a press. The fixture, and the experimental setting are shown in Fig. 9.

Since the rotorcap is cylindrically symmetric, and the offset in grasping along the Z axis is not important in the object handling, we have tested grasping perturbation in 4 directions (see Tab. II). Fig. 12 presents a comparison of the results for the real-world and the simulated scenario. Same as in the magnet experiment case, the plots are smoothed and interpolated between the non-uniform data-points used.

The simulated and the real-world results show a good match, with the simulated version indicating slightly smaller basins of success. The feedback from simulation can be then deemed more restrictive, and should result in more optimal designs with a wide margin of error. The discrepancy between the results is due to the lack of the compliance modelling. The simulated device is rigid, and does not allow the robot to adapt to the forces imposed by the object or the fixture.

C. Application in the Industrial Scenario

After testing the computed fingers in simulation and on a test platform, we were able to confirm that the gripper performs as expected, and is able to compensate for the vision uncertainties involved. The designed gripper fingers were applied in the industrial use-case, in which an electrical motor was assembled. Fig. 10 presents the grasps executed in the industrial setting. The robotic arm used was the Universal Robot model UR-5, which was equipped with a WSG50 gripper. The vision system consisted of the combination of Primesense Carmine sensor and two pike cameras with the projector (see Fig. 10), which has also been used for the uncertainty computations reported in section III-A.

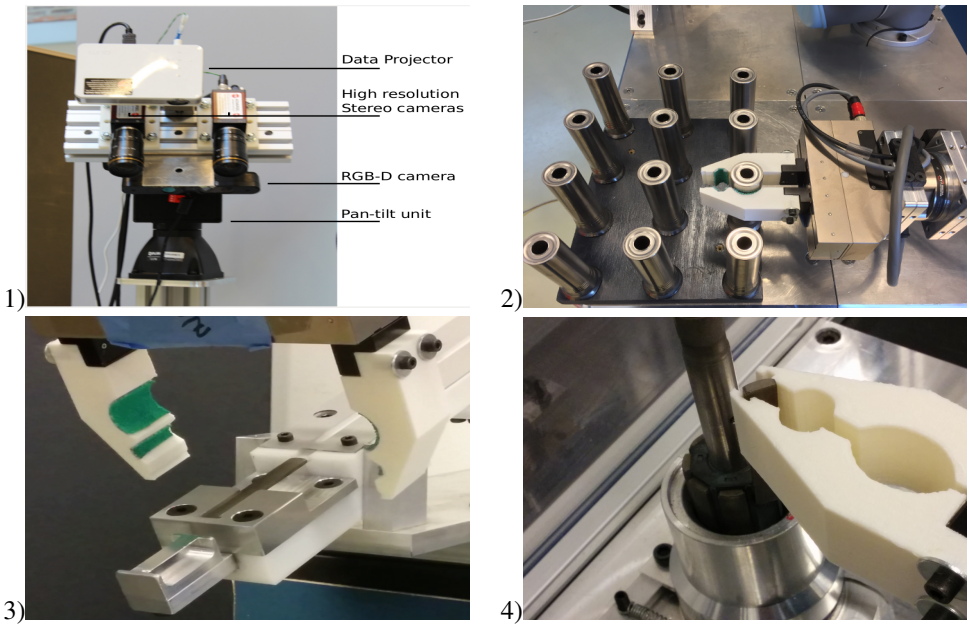

Fig. 10. The application of the computed gripper design in the industrial context. In order: 1) The vision system used, 2) Grasping the rotorcap, 3) Grasping the magnet, 4) Inserting the magnet into the rotorcap assembly.

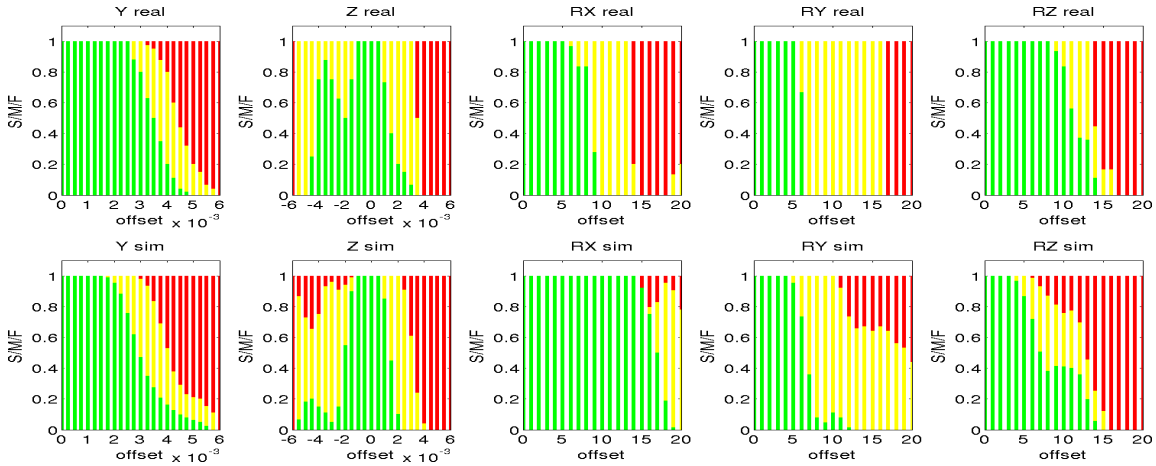

Fig. 11. A comparison between results for the real magnet grasping setup (top) and the simulated experiment (bottom). The bars represent respectively the percentages of: successfull grasps (green), misaligned grasps (yellow), failed grasps (red).

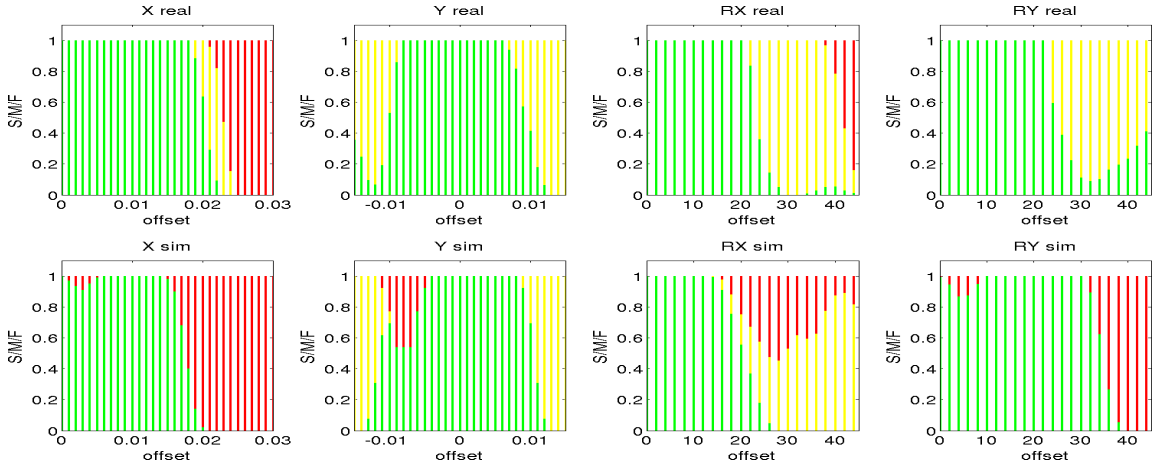

Fig. 12. A comparison between results for the real rotorcap grasping setup (top) and the simulated experiment (bottom). The bars represent respectively the percentages of: successfull grasps (green), misaligned grasps (yellow), failed grasps (red).

V. CONCLUSION

In this paper we have presented an approach to the problem of the optimal gripper design to compensate for the vision system induced pose estimation uncertainties. We have analyzed the errors in vision based pose estimation, and defined these as the task context for our automated simulation-based finger designing procedure. We have computed the optimal geometry of fingers for two objects in a real industrial-based scenario. These geometries have then been merged into a single finger design, that was then used in the experiments executed both in simulation, on a real test platform, and subsequently in a real industrial scenario.

We were able to obtain a decent match between the results from simulation and from the real-world experiments. The few cases in which the outcomes were mis-matched suggest that the feedback obtained from simulation is often more restrictive, and thus results in more robust designs. We argue that by this we can affirm the validity of our proposed methodology.

Still, we are aware that there are sufficient discrepancies between the simulated and real results to justify further development of our simulation environment, and more extensive testing. In our future work we plan to enhance our suite with compliance, and include more elaborate friction models. Furthermore, in our future experiments we plan to test a new physics engine designed for industrial assembly simulation [30].

ACKNOWLEDGMENT

The research leading to these results has received funding from the EU FoF Project ReconCell (project number 680431) and by the Danish Agency for Science, Technology and Innovation, project CARMEN.

REFERENCES

[1] Schunk. (2015) Schunk egrip. [Online]. Available: http://www.schunk-produkte.com/en/tools/3d-designtool-egrip.html

[2] L.-P. Ellekilde and H. G. Petersen, "Design and test of object aligning grippers for industrial applications," in *Intelligent Robots and Systems, 2006 IEEE/RSJ International Conference on*. IEEE, 2006, pp. 5165–5170.

[3] A. Wolniakowski, J. A. Jorgensen, K. Miatliuk, H. G. Petersen, and N. Krüger, "Task and context sensitive optimization of gripper design using dynamic grasp simulation," in *20th International Conference on Methods and Models in Automation and Robotics*, 2015.

[4] G. C. Causey and R. D. Quinn, "Gripper design guidelines for modular manufacturing," in *Robotics and Automation, 1998. Proceedings. 1998 IEEE International Conference on*, vol. 2. IEEE, 1998, pp. 1453–1458.

[5] G. Causey, "Guidelines for the design of robotic gripping systems," *Assembly Automation*, vol. 23, no. 1, pp. 18–28, 2003.

[6] S. Krenich, "Multicriteria design optimization of robot gripper mechanisms," ser. Solid Mechanics and Its Applications. Springer Netherlands, 2004, vol. 117, pp. 207–218.

[7] G. C. Causey, "Elements of agility in manufacturing," Ph.D. dissertation, Case Western Reserve University, 1999.

[8] T. Zhang, "Optimal design of self-aligning robot gripper jaws," Ph.D. dissertation, 2001.

[9] T. Zhang, L. Cheung, and K. Goldberg, "Shape tolerance for robot gripper jaws," in *IEEE/RSJ International Conference on Intelligent Robots and Systems*, 2001, pp. 1782–1787.

[10] M. T. Zhang and K. Goldberg, "Designing robot grippers: optimal edge contacts for part alignment," *Robotica*, vol. 25, no. 03, p. 341, Nov. 2006.

[11] E. Nikandrova and V. Kyrki, "Category-based task specific grasping," *Robotics and Autonomous Systems*, vol. 70, pp. 25–35, 2015.

[12] M. Ciocarlie and P. Allen, "Data-driven optimization for underactuated robotic hands," in *Robotics and Automation (ICRA), 2010 IEEE International Conference on*. IEEE, 2010, p. 12921299.

[13] A. Wolniakowski, K. Miatliuk, N. Krüger, and J. A. Rytz, "Automatic evaluation of task-focused parallel jaw gripper design," in *International Conference on Simulation, Modeling, and Programming for Autonomous Robots*, 2014.

[14] S. M. Olesen, S. Lyder, D. Kraft, N. Krüger, and J. B. Jessen, "Real-time extraction of surface patches with associated uncertainties by means of kinect cameras," *Journal of Real-Time Image Processing*, pp. 1–14, 2012. [Online]. Available: http://dx.doi.org/10.1007/s11554-012-0261-x

[15] A. Belhedi, A. Bartoli, S. Bourgeois, V. Gay-Bellile, K. Hamrouni, and P. Sayd, "Noise modelling in time-of-flight sensors with application to depth noise removal and uncertainty estimation in three-dimensional measurement," *Computer Vision, IET*, vol. 9, no. 6, pp. 967–977, 2015.

[16] A. E. Johnson and M. Hebert, "Using spin images for efficient object recognition in cluttered 3d scenes," *Pattern Analysis and Machine Intelligence, IEEE Transactions on*, vol. 21, no. 5, pp. 433–449, 1999.

[17] A. Frome, D. Huber, R. Kolluri, T. Bülow, and J. Malik, "Recognizing objects in range data using regional point descriptors," in *Computer Vision-ECCV 2004*. Springer, 2004, pp. 224–237.

[18] A. S. Mian, M. Bennamoun, and R. Owens, "Three-dimensional model-based object recognition and segmentation in cluttered scenes," *Pattern Analysis and Machine Intelligence, IEEE Transactions on*, vol. 28, no. 10, pp. 1584–1601, 2006.

[19] R. B. Rusu, N. Blodow, and M. Beetz, "Fast point feature histograms (fpfh) for 3d registration," in *Robotics and Automation, 2009. ICRA'09. IEEE International Conference on*. IEEE, 2009, pp. 3212–3217.

[20] Y. Guo, F. Sohel, M. Bennamoun, M. Lu, and J. Wan, "Rotational projection statistics for 3d local surface description and object recognition," *International journal of computer vision*, vol. 105, no. 1, pp. 63–86, 2013.

[21] L. Kiforenko, A. G. Buch, L. Bodenhagen, and N. Kruger, "Object detection using categorised 3D edges," vol. 9445. SPIE, 2015.

[22] S. Salti, F. Tombari, and L. Di Stefano, "Shot: Unique signatures of histograms for surface and texture description," *Computer Vision and Image Understanding*, vol. 125, pp. 251–264, 2014.

[23] Y. Guo, M. Bennamoun, F. Sohel, M. Lu, and J. Wan, "3d object recognition in cluttered scenes with local surface features: a survey," *Pattern Analysis and Machine Intelligence, IEEE Transactions on*, vol. 36, no. 11, pp. 2270–2287, 2014.

[24] Y. Guo, M. Bennamoun, F. Sohel, M. Lu, J. Wan, and N. M. Kwok, "A comprehensive performance evaluation of 3d local feature descriptors," *International Journal of Computer Vision*, vol. 116, no. 1, pp. 66–89, 2016.

[25] L. Kiforenko, A. G. Buch, and N. Kruger, "Object detection using a combination of multiple 3d feature descriptors." Springer International Publishing, 2015.

[26] M. A. Fischler and R. C. Bolles, "Random sample consensus: A paradigm for model fitting with applications to image analysis and automated cartography," *Communications of the ACM*, vol. 24, no. 6, pp. 381–395, 1981.

[27] C. Ferrari and J. Canny, "Planning optimal grasps," in *IEEE International Conference on Robotics and Automation (ICRA)*, May 1992, pp. 2290–2295.

[28] J. Jorgensen, L. Ellekilde, and H. Petersen, "RobWorkSim - an Open Simulator for Sensor Based Grasping," in *Proceedings of Joint 41st International Symposium on Robotics (ISR 2010) and the 6th German Conference on Robotics (ROBOTIK 2010)*, Munich, 2010, pp. 1–8.

[29] S. J. Wright, "Coordinate descent algorithms," *Mathematical Programming*, vol. 151, no. 1, pp. 3–34, 2015. [Online]. Available: http://dx.doi.org/10.1007/s10107-015-0892-3

[30] T. N. Thulesen and H. G. Petersen, "RobWorkPhysicsEngine: A new dynamic simulation engine for manipulation actions," in *2016 IEEE International Conference on Robotics and Automation (ICRA)*, 2016.